Effect of carbon doping on buffer leakage in AlGaN/GaN high electron mobility transistors

C. Poblenz, P. Waltereit, S. Rajan, S. Heikman, U. K. Mishra, and J. S. Speck

Citation: Journal of Vacuum Science & Technology B: Microelectronics and Nanometer Structures Processing, Measurement, and Phenomena **22**, 1145 (2004); doi: 10.1116/1.1752907

View online: https://doi.org/10.1116/1.1752907

View Table of Contents: https://avs.scitation.org/toc/jvn/22/3

Published by the American Institute of Physics

Effect of carbon doping on buffer leakage in AlGaN/GaN high electron mobility transistors

C. Poblenz,[a] P. Waltereit, S. Rajan, S. Heikman, U. K. Mishra, and J. S. Speck
Department of Materials and Department of Electrical and Computer Engineering, University of California, Santa Barbara, California 93106

(Received 6 February 2004; accepted 29 March 2004; published 24 May 2004)

Carbon doping via CBr_4 in AlGaN/GaN high electron mobility transistors grown by rf-plasma-assisted molecular beam epitaxy on 4H–SiC (0001) was investigated as a means to reduce buffer leakage. For carbon doping in the first 400 nm of the structure, a significant decrease in buffer leakage was observed with increasing overall carbon concentration. A carbon doping scheme in which the level of doping is tapered from $6\times10^{17}\,cm^{-3}$ down to $2\times10^{17}\,cm^{-3}$ was found to result in sufficiently low drain-source leakage currents. The effect of thickness of the GaN:C layer was explored as well as the effect of thickness of the subsequent unintentionally doped GaN layer. For structures with reduced leakage, rf $I-V$ and power measurements revealed better performance in structures in which the two-dimensional electron gas was spaced at a large distance from the GaN:C layer. Possible sources and locations of unintentional free carriers contributing to leakage in these structures are discussed in light of the results. © *2004 American Vacuum Society.*
[DOI: 10.1116/1.1752907]

I. INTRODUCTION

The AlGaN/GaN material system continues to show great potential for the fabrication of high-power microwave transistors. High electron mobility transistors (HEMTs) grown either by metalorganic chemical vapor deposition (MOCVD) or molecular beam epitaxy (MBE) have demonstrated very good power performance in recent years.[1–5] High quality semi-insulating GaN buffer layers are essential for realizing good device performance and sharp current pinch-off in HEMTs. Unintentionally doped (UID) GaN grown by both MOCVD and MBE typically exhibits some degree of *n*-type conductivity, presumably due to unintentional oxygen or silicon doping, which can result in buffer leakage in GaN-based electronic devices.

It is now recognized that the introduction of intentional compensating centers can be a practical route for realizing semi-insulating GaN. In MOCVD-grown GaN, intentional iron doping has been used to produce highly resistive buffers for HEMTs.[6] Recent approaches for producing semi-insulating GaN by MBE have included the introduction of deep levels via carbon doping[7–9] or beryllium doping.[10] Carbon is an interesting impurity in GaN, as it is one of the most common unintentional impurities in the III-nitrides (along with oxygen and hydrogen) and because it may show amphoteric behavior. Recent theory work by Wright,[11] which is supported by experiment,[12] demonstrates that when the Fermi level E_F is close to the conduction band, the formation of the shallow acceptor C_N is favorable for all growth conditions, whereas when E_F is close to the valence band, it is favorable to form either the shallow donor C_{Ga} or a carbon interstitial complex. Since most GaN layers show unintentional *n*-type conductivity, carbon may be a very effective compensating acceptor.

In this work we explore the effect of carbon doping on buffer leakage in AlGaN/GaN HEMT structures grown by rf-plasma-assisted MBE. We have recently shown that CBr_4 is an effective source for carbon doping in GaN MBE growth.[9] Using CBr_4, carbon levels greater than $10^{18}\,cm^{-3}$ can be readily realized without any measurable change of the GaN growth morphology. We have not been able to detect any measurable bromine incorporation in our GaN. In this paper, we demonstrate a significant decrease in buffer leakage for structures including carbon-doped GaN in the buffer structure and begin to explore the subsequent effects of the presence of carbon in the buffer on rf device characteristics.

II. EXPERIMENT

The nitride MBE growth reported here was performed in a Varian Gen II MBE system. The active nitrogen was supplied by an AppliedEpi Unibulb rf-plasma source utilizing ultrahigh purity nitrogen (99.9995% purity), further purified by an inert gas purifier (Aeronex, San Diego, CA) at the rf-plasma source gas inlet. Conventional effusion cells were used to provide the group III elements and carbon was introduced utilizing a CBr_4 gas delivery system (AppliedEpi). Carbon doping levels in the HEMT buffers were determined based on a secondary ion mass spectroscopy (SIMS) calibration sample grown under identical conditions to the HEMT buffers.

The HEMT structures were grown on semi-insulating 4H–SiC substrates commercially available from Cree, Inc. Prior to MBE growth the substrates received a chemical mechanical polish (CMP) treatment by NovaSiC, Inc. A 0.5 μm titanium film was deposited on the backside of the wafer to provide efficient heat transfer. Quarter-wafer pieces of the substrate were mounted for growth on molybdenum sample holders. The substrate temperature was monitored by an optical pyrometer and the readings were calibrated to the temperature dependence of Ga desorption.[13]

[a]Electronic mail: cpoblenz@engineering.ucsb.edu

Before growth, the substrates were exposed to three cycles of Ga deposition and desorption to clean the surface from oxides.[14,15] The growth was initiated with a 45 nm AlN nucleation layer deposited at ~740 °C with a III/V ratio close to Al droplet formation. The surface of the AlN grown under these conditions was smooth and showed a characteristic monolayer high step-terrace structure. Temperature variations over the sample resulted in Al droplets in cooler areas and no droplets in hotter areas. After AlN growth, with the Al and N shutters both closed, the substrate temperature was reduced to ~715 °C and GaN growth was initiated. A two-step growth scheme was used to control dislocation density in a similar manner as reported by Manfra *et al.*[16] We have established a buffer growth scheme that allows us to achieve reproducible dislocation densities on the order of $2-3\times10^{10}\,\mathrm{cm}^{-3}$, as determined by plan view transmission electron microscopy (TEM). Further details on our buffer growth will be published elsewhere.[17] Finally, a 30 nm thick $Al_{0.30}Ga_{0.70}N$ cap was deposited. The samples were analyzed using high resolution x-ray diffraction and the cap composition was calculated based on the peak separation between the GaN and AlGaN peaks in $2\theta-\omega$ scans, assuming coherently strained AlGaN layers.[18] As the samples were grown near the crossover from the intermediate to Ga-droplet regime,[13] small temperature variations over the sample typically resulted in the formation of Ga droplets in some areas of the sample. Excess Ga and droplets were etched off post-growth using HCl.

HEMT structures with a drain-source spacing of 3.4 μm, a gate length of 0.7 μm, and gate width of 150 μm were fabricated utilizing standard processing steps. Ohmic contacts consisting of a Ti/Al/Ni/Au metal stack were deposited and alloyed at 870 °C in a nitrogen atmosphere. Mesa isolation was performed using a BCl_3/Cl_2 reactive ion etch, then Ni/Au/Ni gates were deposited. Finally, the samples were passivated using SiN deposited by plasma-enhanced CVD and contacts were made to the source, gate, and drain by etching the SiN in a CF_4 plasma. Hall test patterns were not fabricated on the samples discussed in this article, although samples grown under similar conditions exhibited Hall mobilities in excess of 1400 $\mathrm{cm}^2/\mathrm{V\,s}$ and sheet carrier concentrations of $\sim1\times10^{13}\,\mathrm{cm}^{-2}$. Buffer leakage was studied by measurement of drain-source $I-V$ curves on isolation patterns consisting of HEMT structures with the two-dimensional electron gas (2-DEG) etched away at the gate region. We report the drain-source voltage necessary to realize 1 mA/mm drain-source current on the etched isolation patterns. This leakage current was chosen as a point of comparison because it is three orders of magnitude lower than typical 2-DEG currents (1 A/mm), and thus is sufficiently low for device operation. To take into account changes in growth conditions across the sample due to variations in substrate temperature, several isolation patterns were measured across each sample and the average result is reported.

III. RESULTS

Three identical structures were grown to investigate the impact of carbon doping level on buffer leakage, as shown in Fig. 1(a). The GaN:C layer in each structure was split into three regions [labeled "A," "B," and "C" in Fig. 1(a)] over which the carbon doping level was sequentially decreased. The thickness of each GaN:C layer was held constant at 100, 200, and 100 nm for regions A, B, and C, respectively. The thickness of the UID-GaN layer was also held constant at 300 nm, giving a total structure thickness of 0.7 μm. Figure 1(b) shows the drain-source $I-V$ curves from isolation patterns on each sample in this study, with carbon doping levels in each layer [in reference to Fig. 1(a)] indicated in the figure. A significant decrease in leakage current was observed with increasing carbon concentration. The voltage at which 1 mA/mm of leakage current is reached was <5 V in the sample with the lowest overall level of carbon doping, which is similar to undoped structures. (Capacitance–voltage mea-

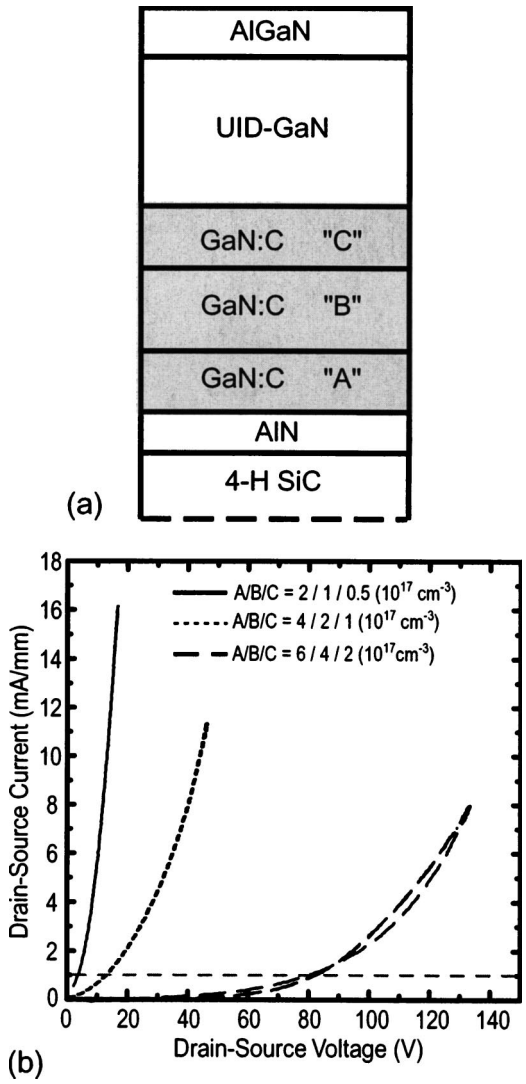

FIG. 1. (a) Representative HEMT structure with GaN:C (shaded area) included in the buffer, where "A" (100 nm thick), "B" (200 nm thick), and "C" (100 nm thick) denote layers with varying levels of carbon doping. The UID-GaN layer thickness was 300 nm. The doping levels for each layer are indicated by the sample in (b). (b) Dependence of the drain-source leakage current on the carbon doping level. The dashed line is a guide for the eye representing 1 mA/mm of leakage current as a point of comparison between samples.

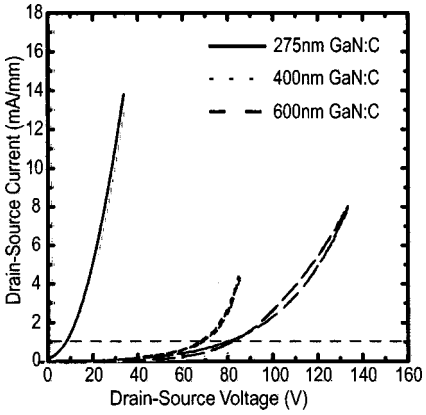

FIG. 2. Dependence of drain-source leakage current on the thickness of the GaN:C layer. The dashed line is a guide for the eye representing 1 mA/mm of leakage current as a point of comparison between samples.

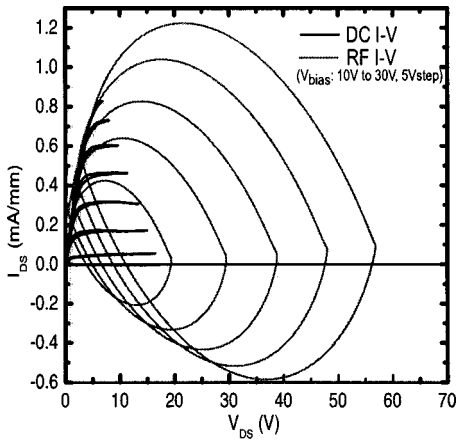

FIG. 4. 4 GHz rf $I-V$ curves for the HEMT structure with 1 μm UID-GaN above the GaN:C layer demonstrating negligible knee walkout.

surements on UID HEMTs with identical structures revealed a UID doping level in the mid-$10^{15}\,\mathrm{cm}^{-3}$ range.) By increasing to the highest overall level of carbon doping, this voltage was increased to 80 V.

The impact of the total thickness of the GaN:C layer on leakage was also investigated and the results are shown in Fig. 2. The sample structures were similar to the schematic in Fig. 1(a), with a sequentially decreasing carbon doping level from 6×10^{17} to $2\times10^{17}\,\mathrm{cm}^{-3}$ over three layers A, B, and C, and a constant 300 nm of UID-GaN grown on top. The thicknesses of layers A, B, and C were kept at a constant ratio of 1:2:1. The total thickness of carbon doped material was varied from 275 to 600 nm and the drain-source leakage was again measured on isolation patterns. As shown in Fig. 2, the sample with the thinnest GaN:C layer had the highest leakage, measuring 1 mA/mm at only 5 V. In contrast, the two samples with thicker GaN:C layers did not yield 1 mA/mm leakage current until 75–80 V bias was applied.

Using the GaN:C buffer structure that exhibited the lowest leakage from Fig. 1(b), the impact of the thickness of UID-GaN on buffer leakage was then investigated. Structures were grown with 0.3 and 1 μm of UID-GaN on top of the GaN:C layer and the results of leakage measurements on isolation patterns are shown in Fig. 3. As demonstrated in the figure, 1 mA/mm leakage current was not reached until >80 V was applied to either sample. Since the leakage current did not increase even when measuring through 1 μm of UID-GaN material, this indicates that the GaN:C layer employed in this structure was sufficient to overcome unintentional doping in the structure. Because both structures exhibited similarly good dc leakage characteristics, the effect of proximity of the GaN:C layer to the 2-DEG interface was then investigated through rf $I-V$ and power measurements. In the sample with 0.3 μm UID-GaN beneath the 2-DEG, power measurements at 4 GHz and a drain bias of 35 V yielded an output power density of 4.2 W/mm with a power-added efficiency (PAE) of 19.5%. In addition, 4 GHz rf $I-V$ curves showed significant knee walkout. In the sample with 1 μm UID-GaN beneath the 2-DEG, power measurements at 4 GHz and a drain bias of 35 V revealed an output power density of 6.6 W/mm with a PAE of 57%.[19] The 4 GHz rf $I-V$ measurements for this sample are shown in Fig. 4, demonstrating negligible knee walkout. This is still under further investigation, but at present we attribute this reduction in knee walkout to reduced buffer dispersion as a result of the increased distance from the GaN:C layer to the 2-DEG interface. At 10 GHz and a drain bias of 40 V, this device exhibited an output power density of 7.3 W/mm and a PAE of 36%.[19]

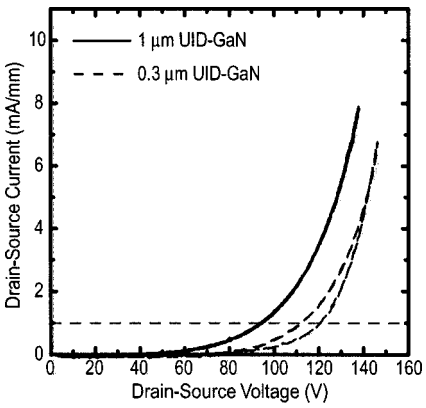

FIG. 3. Dependence of drain-source leakage current on the thickness of the UID GaN with the same underlying GaN:C buffer. The dashed line is a guide for the eye representing 1 mA/mm of leakage current as a point of comparison between samples.

IV. DISCUSSION

The difficulty in combating buffer leakage in direct-grown HEMT structures is that the magnitude and origin of the unintentional free carriers in the structure are not well known. Unintentional free carriers may form in the GaN near the interface with the underlying AlN or the full buffer layer having residual free carriers. The aim and design of these experiments was therefore twofold: to reduce buffer leakage via carbon doping and to clarify the possible origin and magnitude of unintentional free carriers. Figure 1(b) demonstrates that for carbon doping over 400 nm at the beginning

of the structure, leakage was not significantly reduced until a tapered carbon scheme beginning at a doping level of $6\times10^{17}\,\mathrm{cm}^{-3}$ of carbon doping was used. It is also interesting to note from this figure that the large improvement in the observed dc $I-V$ characteristics corresponded to a relatively small change in the carbon doping level (from 2×10^{17} to $6\times10^{17}\,\mathrm{cm}^{-3}$ initial doping levels). Preliminary data from samples doped with higher, constant carbon levels had essentially identical leakage characteristics to those with tapered carbon doping profiles. Figure 2 demonstrates that at least 400 nm of carbon-doped material must be used to suppress leakage. Increasing the thickness of GaN:C beyond 400 nm did not change the leakage characteristics. Collectively, from this data alone, we cannot conclude whether the free carriers responsible for the leakage are associated with GaN near the GaN/AlN interface or are continuously distributed throughout the GaN buffer.

The results shown in Fig. 3, however, suggest that the free carriers originate near the GaN/AlN interface. If the UID-GaN was extremely leaky (e.g., exhibiting 1 mA/mm leakage current at 5 V bias), we would expect to measure higher leakage currents after growth of 1 μm of UID material, and this was not observed. To further test this idea, structures were grown in which the carbon doping level was increased to $8\times10^{17}\,\mathrm{cm}^{-3}$ but only the first 100 nm of GaN were doped. These structures were capped with 0.7 μm of UID-GaN. Measurements of isolation patterns yielded 1 mA/mm of leakage current at >80 V. This is consistent with the charge compensation occurring near the GaN/AlN interface and not persisting into the UID-GaN.

Although this result indicates that free carriers in the GaN buffer originate near the GaN/AlN interface, there are still several possibilities of the source of the unintentional dopants. The SiC surface, even after several cycles of Ga adsorption and desorption, may have had residual impurities that subsequently floated on the growing crystal surface and acted as a source of oxygen or silicon donors in the AlN or GaN layers. The AlN was grown under Al-rich conditions, near the transition for Al droplet formation. In our growths, we directly transitioned to GaN growth after AlN growth. Residual Al on the growth surface will be incorporated in preference to Ga in a growing III-nitride layer and thus we may have a Ga-rich AlGaN layer near the nominal GaN/AlN interface. In our previous work, we have shown that AlGaN has markedly higher oxygen affinity than GaN, even under growth with a complete Ga bilayer.[20] Other groups have also studied the dependence of buffer leakage on the Al/N flux ratio during the growth of AlN nucleation layers. Initial results indicate that Al-rich growth of the AlN can result in leaky GaN buffers.[21]

V. CONCLUSION

In conclusion, carbon doping via CBr_4 has been implemented into buffer structures for high quality HEMTs grown directly on 4H–SiC by MBE. With an appropriate growth structure, we have shown that carbon can be effective in reducing buffer leakage. For carbon doping in the first 400 nm of the structure, a significant decrease in buffer leakage was observed with increasing overall carbon concentration. In such structures, a carbon doping scheme in which the doping level was tapered from $6\times10^{17}\,\mathrm{cm}^{-3}$ down to $2\times10^{17}\,\mathrm{cm}^{-3}$ resulted in sufficiently low drain-source leakage currents (i.e., 1 mA/mm at 80 V bias). For this carbon doping scheme, ~400 nm of GaN:C was also established as the minimum thickness necessary to sufficiently reduce leakage. The free carriers responsible for leakage were apparently located within at least the first 100 nm of the structure based on the observation that the leakage did not change with growth of up to 1 μm of UID-GaN on top of GaN:C structures. Preliminary rf $I-V$ and power measurements demonstrated improved performance, however, in those structures in which the GaN:C layer is spaced farther away from the 2-DEG interface. An output power density of 7.3 W/mm (36% PAE) at 10 GHz and 40 V drain bias was achieved for such a structure with little evidence of knee walkout in rf $I-V$ curves.

ACKNOWLEDGMENTS

The authors acknowledge financial support from DARPA (Edgar Martinez, Program Manager) managed by the ONR (Harry Dietrich, Contract Monitor), and from the AFOSR (Gerald Witt, Program Manager). This work made use of the MRL Central Facilities supported by the MRSEC Program of the National Science Foundation under Award No. DMR00-80034. The authors would also like to thank Tom Mates for help with SIMS experiments.

[1]H. Xing, S. Keller, Y. F. Wu, L. McCarthy, I. P. Smorchkova, D. Buttari, R. Coffie, D. S. Green, G. Parish, S. Heikman, L. Shen, N. Zhang, J. J. Xu, B. P. Keller, S. P. DenBaars, and U. K. Mishra, J. Phys.: Condens. Matter **13**, 7139 (2001).
[2]R. Behtash, H. Tobler, M. Neuburger, A. Schurr, H. Leier, Y. Cordier, F. Semond, F. Natali, and J. Massies, Electron. Lett. **39**, 626 (2003).
[3]J. S. Moon, M. Micovic, P. Janke, P. Hashimoto, W.-S. Wong, R. D. Widman, L. McCray, A. Kurdoghlian, and C. Nguyen, Electron. Lett. **37**, 528 (2001).
[4]D. S. Katzer, S. C. Binari, D. F. Storm, J. A. Roussos, B. V. Shanabrook, and E. R. Glaser, Electron. Lett. **38**, 1740 (2002).
[5]N. Weimann, M. J. Manfra, and R. Wachtler, IEEE Electron Device Lett. **24**, 57 (2003).
[6]S. Heikman, S. Keller, S. P. DenBaars, and U. K. Mishra, Appl. Phys. Lett. **81**, 439 (2002).
[7]H. Tang, J. B. Webb, J. A. Bardwell, S. Raymond, J. Salzman, and C. Uzan-Saguy, Appl. Phys. Lett. **78**, 757 (2001).
[8]J. B. Webb, H. Tang, S. Rolfe, and J. A. Bardwell, Appl. Phys. Lett. **75**, 953 (1999).
[9]D. S. Green, J. S. Speck, and U. K. Mishra (submitted for publication).
[10]D. S. Katzer, D. F. Storm, S. C. Binari, J. A. Roussos, B. V. Shanabrook, and E. R. Glaser, J. Cryst. Growth **251**, 481 (2003).
[11]A. F. Wright, J. Appl. Phys. **92**, 2575 (2002).
[12]C. H. Seager, A. F. Wright, J. Yu, and W. Götz, J. Appl. Phys. **92**, 6553 (2002).
[13]B. Heying, R. Averbeck, L. F. Chen, E. Haus, H. Riechert, and J. S. Speck, J. Appl. Phys. **88**, 1855 (2000).
[14]O. Brandt, R. Muralidharan, P. Waltereit, A. Thamm, A. Trampert, H. von Kiedrowski, and K. H. Ploog, Appl. Phys. Lett. **75**, 4019 (1999).
[15]S. Wright and H. Kroemer, Appl. Phys. Lett. **36**, 210 (1980).
[16]M. J. Manfra, N. G. Weimann, J. W. P. Hsu, L. N. Pfeiffer, K. W. West, and S. N. G. Chu, Appl. Phys. Lett. **81**, 1456 (2002).

[17]P. Waltereit, C. Poblenz, S. Rajan, F. Wu, J. S. Speck, and U. K. Mishra (submitted for publication).
[18]A. Saxler, P. Debray, R. Perrin, S. Elhamri, W. C. Mitchel, C. R. Elsass, I. P. Smorchkova, B. Heying, E. Haus, P. Fini, J. P. Ibbetson, S. Keller, P. M. Petroff, S. P. DenBaars, U. K. Mishra, and J. S. Speck, J. Appl. Phys. **87**, 369 (2000).
[19]S. Rajan, P. Waltereit, C. Poblenz, S. J. Heikman, D. S. Green, J. S. Speck, and U. K. Mishra, IEEE Electron Device Lett. **25**, 247 (2004).
[20]C. R. Elsass, T. Mates, B. Heying, C. Poblenz, P. Fini, P. M. Petroff, S. P. DenBaars, and J. S. Speck, Appl. Phys. Lett. **77**, 3167 (2000).
[21]D. F. Storm, D. S. Katzer, S. C. Binari, and B. V. Shanabrook (unpublished).